LEGIBILITY NOTICE

A major purpose of the Technical Information Center is to provide the broadest dissemination possible of information contained in DOE's Research and Development Reports to business, industry, the academic community, and federal, state and local governments.

Although a small portion of this report is not reproducible, it is being made available to expedite the availability of information on the research discussed herein.

LA-UR -89-3268

NOV 0 1989

Los Alamos National Laboratory is operated by the University of California for the United States Department of Energy under contract W-7405-ENG-36

LA-UR--89-3268

DE90 002354

TITLE: A HIGH-SPEED BEAM OF LITHIUM DROPLETS FOR COLLECTING DIVERTED ENERGY AND PARTICLES IN ITER

AUTHOR(S): K. A. Werley

SUBMITTED TO: The 13th Symposium on Fusion Engineering (IEEE), Knoxville, Tennessee, HYatt Regency Hotel, October 2-6, 1989.

A HIGH-SPEEED BEAM OF LITHIUM DROPLETS FOR COLLECTING DIVERTED ENERGY AND PARTICLES IN ITER[1]

K. A. Werley, Los Alamos National Laboratory, Los Alamos, NM 87545

Abstract: A high-speed ($160 m/s$) beam ($0.14 \times 0.86 m$) of liquid-lithium droplets passing through the divertor region(s) below (and above) the main plasma has the potential to replace and out-perform "conventional" solid divertor plates in both heat and particle removal. In addition to superior heat-collection properties, the lithium beam would: (1) remove impurities; (2) require low power to circulate the lithium; (3) exhibit low-recycle divertor operation compatible with lower-hybrid current drive, H-mode plasma confinement, and no flow reversal in the edge plasma; (4) be insensitive to plasma shifts; and finally (5) protect solid structures from the plasma thermal energy for those disruptions that deposit energy preferentially into the divertor while simultaneously being rapidly re-established after a major disruption. Scoping calculations identifying the beam configuration and the droplet dynamics, including formation, MHD effects, gravitational effects, thermal response and hydrodynamics, are presented. Limitations and uncertainties are also discussed.

INTRODUCTION

A critical issue for the International Thermonuclear Experimental Reactor (ITER) is the successful removal of the high heat and particle fluxes leaving the core plasma. The base-case design[1] proposes the use of a double-null poloidal-field divertor that operates in a low wall-density regime in order to be consistent with the H-mode confinement and lower-hybrid current drive. Large heat fluxes, erosion rates, and stresses require the use of special techniques and geometries, such as tilted or rotating collector plates and magnetically sweeping the diverted plasma across the divertor collector plate. Even with these techniques, the plate heat flux (15-25 MW/m^2)[1] and the gross sputtering rate ($\sim 2 m/yr$) are high.[1] Adding to these requirements the need to accommodate disruptions and edge-localized modes (ELMs) brings into question the feasibility and reliability of operating clean ($Z_{eff} < 2.0$), steady-state thermonuclear plasmas using "conventional" divertor plates.

Historically, suggestions to alleviate heat flux and particle removal problems include: (1) eliminating divertor plate erosion and stresses by protecting it with a renewable liquid film; and (2) using hydride-forming surfaces (titanium for example) to remove hydrogen particles. Both of these approaches have drawbacks. The residence time for renewable films is necessarily short to limit temperature and associated vapor pressure to acceptable levels. Also, surfaces become saturated with hydrogen and must be replaced and regenerated at elevated temperature (800-1000°C) for several hours.

A suggestion which ostensibly combines the best features of these two approaches while eliminating the drawbacks is that of a gravity-driven lithium flow down a screen[2] or flat plate[3]. Lithium acts as a getter material, forming lithium-hydride and hopefully would flow sufficiently fast for adequate heat removal without serious evaporation. However, the electric current, induced by moving a conducting fluid across a magnetic field, produces a $\vec{J} \times \vec{B}$ force that resists the fluid motion. Wells[4] concludes that gravity-driven flow down a screen or wall cannot move sufficiently fast to remove the heat in the presence of the MHD forces expected in a tokamak fusion reactor.

The above-mentioned MHD effects are greatly reduced[1] by dividing the lithium into small droplets to eliminate the return path for electric currents. The lithium droplets would be formed by the breakup of a lithium jet after leaving a nozzle. The "beam" of accelerated droplets (or "driven rain") that is formed by an array of such nozzles could form the basis of a lithium-droplet divertor collector plate. The resulting lithium droplet collector, as described in Table I, has good engineering features with many significant advantages over conventional divertor-plate designs. For example, a lithium-droplet beam (LDB) can accommodate higher particle- and energy-flux peaking than a solid wall while simultaneously eliminating hot spots and stresses. A simplicity in design results, which permits ease of maintenence and excellent reliability, particularly when disruption effects are considered. In addition, MHD-induced liquid-metal pumping losses are avoided and vacuum pumping power consumption is lowered. Furthermore, the LDB concept can be applied to widely varying systems by adjusting the droplet size, spacing, and velocity across the beam dimensions.

The LDB also scheme exhibits important, ITER(tokamak)-specific advantages, including relative insensitivity to plasma shifts and an ability to recover and to protect solid structures from diverted energy associated with disruptions and ELMs. The LDB is also inherently a low-recycle divertor, and, therefore, it should be compatible with (1) lower-hybrid current drive, (2) H-mode operation; and (3) operation with no particle flow reversal in the edge plasma.

Limitations are also noted in Table I. First, safety problems are associated with working with liquid metals and the need for isolation from water. Secondly, limitations on the lithium temperature exist, details of which are described in later sections. The LDB scheme also has some unknowns associated with its ability to pump helium and neutral hydrogen isotopes, as well as the feasibility and cost of Li-H (D,T) separation.

TABLE I. Features of a Lithium-Droplet Divertor Collector

Engineering Features:

- Coupled particle and energy collection (e.g., hydride formation)
- Small overall size with "extended" lithium surface
  - can handle large particle fluxes of deuterium,
  - can handle high surface energy fluxes,
  - can tailor spatial distribution of lithium-droplet velocity
- No thermal or pressure stress problems of a "conventional" divertor
- Elimination of hot spots
- Ease of maintenance
- Negligible lithium-circulation MHD pressure drop)
- Significant reduction in required vacuum pump power
- Higher-Z impurity removal
- Lithium is a low-Z plasma impurity

Special Features:

- Insensitive to plasma shifts
- Can survive disruptions moving into the divertor, fast post-disruption recovery
- Low plasma-particle recycle, therefore, should be compatible with
  - Lower hybrid current drive,
  - H-mode plasma confinement,
  - No particle flow reversal in the scrape-off
- Passive, recoverable, self-limiting plasma shutdown mechanism

Limitations:

- Safety considerations of pressurized liquid metals (limited quantity)
- Freezing, vaporization, and hydrogen retainability temperatures

Unknowns:

- Ability to remove helium ash and other impurities
- Tritium separation technologies and costs
- Feasibility of droplet collection
- Pre beam jet start up and transient effects (e.g., spillage)

---

[1]Work supported by US DOE, Office of Fusion Energy

This report examines details of the LDB collector as applied to ITER. First, the general configuration is presented, followed by descriptions of the individual droplet dynamics and the global size and hydrodynamic properties of the lithium. Characteristics of the LDB are then summarized and interim conclusions are given. It is noted that Reid, Wells, et al.,[6] of ORNL first proposed using a lithium rain scheme with bundle divertors for the TNS device, and subsequently, this scheme was proposed[7,8] as a thermal energy dump for a field-reversed mirror reactor. A similar jet system has been suggested as a liquid metal limiter and has been tested on a tokamak experiment.[13]

LITHIUM-DROPLET-BEAM (LDB) CONCEPT DEVELOPMENT

SYSTEM CONFIGURATION

The proposed LDB configuration, as applied to ITER, is illustrated in Figures 1-3. Several different views are required to described adequately the inherently three-dimensional nature of the combined LDB and tokamak systems. The lithium beam is sketched onto drawings of ITER taken from Ref. 1.

The lithium droplets are formed by forced turbulent-jet flow of liquid lithium through a nozzle array. The lithium leaving each nozzle breaks up into droplets, and the resulting LDB enters the magnetic field, passes through the tokamak divertor accumulating diverted plasma particles and kinetic energy, and then leaves the tokamak and is collected in a tank. The droplet formation and collection are done external to the tokamak in a region of low magnetic field so that MHD-induced pressure drops associated with circulating a conducting fluid is negligible. The collected liquid lithium is circulated through a heat exchanger and a lithium-hydride separator (e.g., molten-salt extractor) before being returned to the injector nozzle. While only one beam is sketched in Figures 1-3, the following calculations assume a single-null divertor with two parallel LDBs passing through the diverted magnetic field lines. A double-null configuration would require an LDB to pass through each divertor. Finally, it is noted that other magnetic and beam configurations are possible, (e.g., vertical LDBs with a single-null outboard divertor, etc.).

DROPLET DYNAMICS

Before discussing the LDB, per se, the properties of an individual lithium droplet are estimated. Since the shape of the beam cross section plays a minor role in the LDB concept, the plasma-LDB interaction region is modelled as a rectangular parallelepiped, as is shown in Figure 4. The sides of the interaction region have a length L_s in the direction of the beam velocity and a height H such that the cross sectional area $A_s = HL_s$ defines the beam/plasma interaction area. The LDB width, W, is needed to define the interaction volume. The length of a field line in the beam plasma interaction region is given by $W/\cos\theta$, where θ is approximately given by the angle between a field-line and the vector $\vec{A}_s$. Assuming that the droplets are equally sized and evenly spaced throughout the volume, the interaction zone is divided into differential volumes of length, l, height, h, and width, w, each containing one spherical droplet of diameter d. This volume, which is illustrated in Figure 4, is used to describe MHD, gravitational, and thermal effects for a given droplet.

Droplet Formation: Lithium droplets are formed in a region of low magnetic field by turbulent-jet flow through a long nozzle which breaks up the lithium into droplets. Tau-Fang Chen and J. R. Davis[14] describe jet break up into a string of evenly spaced droplets with a size about equal to the nozzle bore. R. E. Phinney[15] provides a formula for estimating the average break-up length, b, in terms of, the nozzle diameter, d, the Ohnesorge number, Z, and the Weber number, We: $b = d\lambda(1+3Z)\sqrt{We}$. The stability parameter, λ, is measured experimentally[7] as a function of the Reynolds number, Re. Values of the other constants are listed in Table II. For $d = 0.005m$ and $v = 100m/s$, then $Re = 10^6$ and $\lambda = 10$, which gives a break-up length of $b = 2.1m$.

MHD Drag, Deflection, and Deformation: When an electrically conducting object crosses a magnetic field electric currents are induced, which interact with the background field producing a range of forces on the object. A net drag force is produced which tends to decelerate the object. Also, curvature terms in the background field cause the object to deflect sideways. Finally, local variation in the forces around the surface of the object tend to deform the object. These effects are described by Welker and Wells[16] and are calculated below.

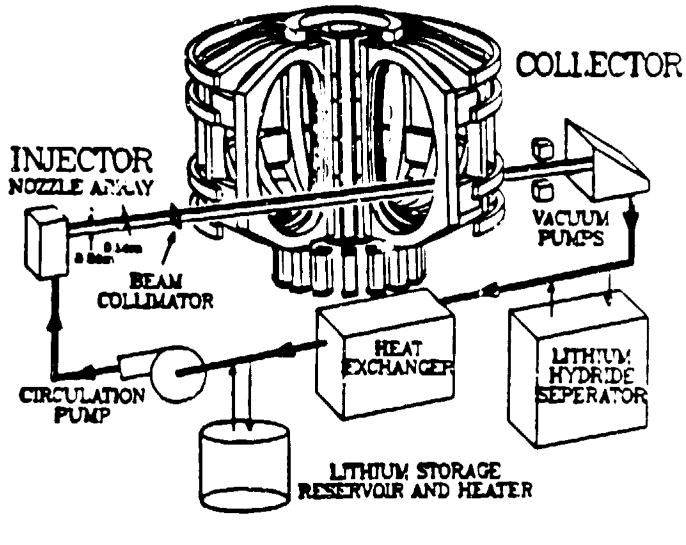

Fig. 1. Schematic of the LDB heat and particle collector drawn onto a view of the magnetic system assembly for ITER.[1]

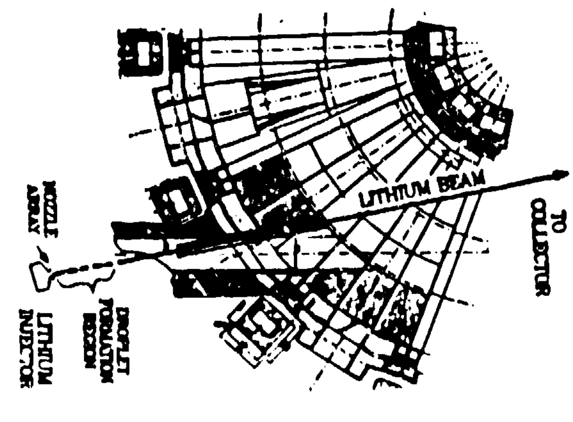

Fig. 2. Lithium-droplet beam projected up into the equatorial plane cross sectional view of ITER.[1] Note that the beam is actually located below the equatorial plane.

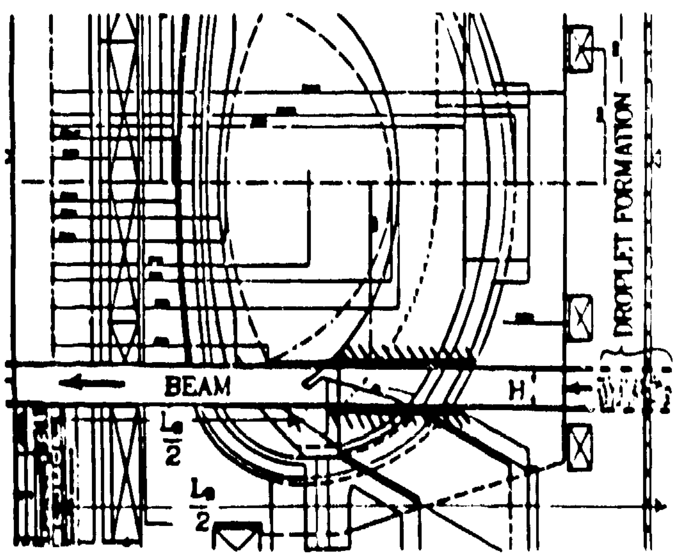

Fig. 3. Lithium droplet beam projected onto a poloidal cross section of ITER.[1] Note that the beam actually lies above the plane of the page.

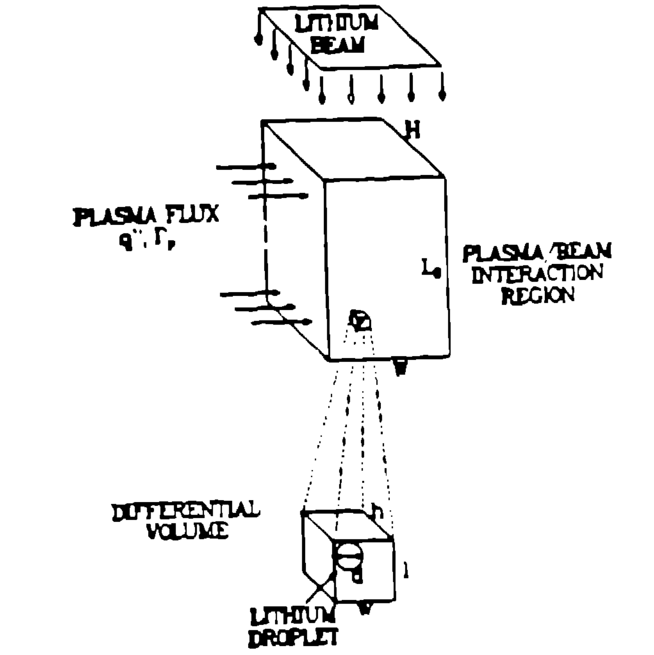

Fig. 4. Model of the LDB-plasma interaction zone and a differential volume element containing a single droplet

TABLE II. Liquid Lithium Properties

resistivity, $\eta = 3.5 \times 10^{-7} ohm - m$	surface tension, $\sigma = 0.365 N/m$
heat capacity, $c_p = 4190 J/kgK$	viscosity, $\mu = 4 \times 10^{-4} Pa - s$
thermal conductivity, $k = 46 W/mK$	density, $\rho = 500\ kg/m^3$
thermal diffusivity, $\alpha = 2.2 \times 10^{-5} m^2/s$	melting point, $T_{mp} = 186°C$

Walker and Wells[8] estimate the reduction in speed, Δv, and the drag force, F_D, experienced as a conducting sphere crosses a magnetic field. The following expressions result

$$\Delta v = \frac{-(\pi d B)^2}{160 \rho \eta L_g}, \tag{1}$$

$$F_D = m\frac{\Delta v}{\Delta t} = \rho\frac{\pi}{6}d^3 \Delta v \frac{v}{L_g} \tag{2}$$

The peak magnetic field is assumed to be $B = 5T$ and a droplet is assumed to experience a linear magnetic field gradient with a scale length of $L_g = 2m$. Equation 2 gives a speed reduction of $\Delta v = 0.011 m/s$, and $F_D = 2.8 \times 10^{-4} N$, which is much less than the surface tension, $F_s = \pi d\sigma = 5.7 \times 10^{-3} N$. Therefore, the MHD drag force has a negligible effect on droplet speed for small droplets, and the droplet will not disintegrate because of MHD drag forces experienced along the trajectory.

The sidewards deflection of a droplet in the direction of the magnetic field caused by the magnetic field curvature is given as follows:[18]

$$\Delta y = \frac{a^1 L_g^2 T (B/L_g)^3}{20 \rho r B \eta} \tag{3}$$

For ITER parameters, $\Delta y \approx 10^{-10} m$ and is negligible. In addition to the MHD deflection force, droplets will charge up via the high speed electrons forming an electrostatic sheath. The resulting pellet gyro-orbit deflection is also negligible.

The magnitude of deformation of the droplet caused by $\bar{J} \times \bar{B}$ forces is estimated[18] by taking the ratio of the MHD pressure drop across the droplet surface, Δp, to the surface tension, p_s, that tends to maintain a spherical droplet. The ratio is given by

$$\frac{\Delta p}{p_s} = \frac{d^3 v B^2}{64 \sigma \eta L_g}, \tag{4}$$

which is ~30 for ITER parameters. This result suggests strong deformation of the droplet would occur, possibly breaking up the droplets into smaller droplets with $\Delta p/p_s \sim 1$ and the original diameter d reduced by $\sqrt[3]{30}$ to ~1.6mm. Another possibility is that the $\bar{J} \times \bar{B}$ force would induce strong internal flow patterns within the droplet. Further examination is required to understand the consequences of the high deformation regime.

Gravitational Deflection: For the configuration envisaged (Figure 1), the lithium droplets move primarily horizontally with speed v. The vertical deflection caused by gravity is given by $z = 0.5gt^2 + v_{z_0}t + z_0$, where z gives the vertical position of the droplet, z_0 specifies the nozzle vertical position, and v_{z_0} is the initial vertical speed. Assuming that v_{z_0} is positive (upward) and that the droplet is collected at a time t_c that is greater than v_{z_0}/g, then the highest the droplet reaches, z_{high}, occurs at $t_{high} = v_{z_0}/g$. The low point, z_{low}, is assumed to occur at the collector where $t_{low} = L_B/v$. The change in height is given by

$$\Delta z = z_{high} - z_{low} = \frac{g}{2}\left[\left(\frac{L_B}{v}\right)^2 - \left(\frac{v_{z_0}}{g}\right)^2\right] - v_{z_0}\left(\frac{L_B}{v} - \frac{v_{z_0}}{g}\right). \tag{5}$$

A symmetric trajectory with z_{high} occurring at the flight mid-point at $v_{z_0}/g = L_B/2v$ minimizes $\Delta z = g/8(L_B/v)^2$. If the distance the beam travels is estimated as double the sum of (a) the major diameter, (b) the field gradient entrance distance, and (c) the break-up length, $L_B = 2 \bullet (2R_T + L_g + b)$, then $L_B = 30m, v_{z_0} = 0.92 m/s$ and $\Delta z = 0.042m$; note that for speeds below $v = 160\ m/s$, Δz could grow large for devices as large as ITER. Since both the MHD and gravitational deflection are small, they have been neglected at this level of design. It is conceivable that some design configurations could capitalize on deflection forces by (1) conforming the beam to the plasma surface, thereby reducing the required beam cross-sectional area or (2) bending the beam to avoid intersecting structure within the reactor.

Droplet Temperature: The thermal evolution of the droplet and its ability to remove heat are crucial to the LDB concept. The average temperature rise in the droplet, ΔT_{AV}, after a time, $t_s = L_s/v$, spent under the maximum heat flux, q'', is calculated from enthalpy balance to be $\Delta T_{AV} = (3L_s/2c_p\rho d)(q''/v)$, can be controlled by choosing the fluid velocity. The heat flux impinging on the lithium is estimated from $q'' = 0.2P_F(1 - f_{RAD})/2N_B A_s$. The calculation uses a major radius of the ITER Technology Phase[1] plasma of $R_T = 5.5m$. The fusion power is assumed to be $P_F = 670 MW$. The radiation fraction is taken as $f_{RAD} = 0.3$, the number of beams is $N_B = 2$, and the area of the source is $A_s = L_s H \simeq 5.0 m^2$ for $L_s \simeq R_T$ and $H \simeq 0.9m$. These parameters give $q'' = 4.7 \times 10^6 W/m^2$.

Approximating the droplet as a solid sphere positioned in a directed uniform heat flux, the spatial and temporal temperature distribution within the droplet is given in Figure 5.[17] This conservative model overestimates peak temperatures by ignoring radiative losses, droplet spinning, and internal convection. Since $\tau = 4\alpha t_s/d^2 = 4\alpha L_s/d^2 v = 0.12$, $f(1, 0, \tau) = 0.4$, and the maximum droplet temperature is given by

$$T_{MAX} = \frac{0.4d}{2k}q'' + \Delta T_{AV} + T_{IN}. \tag{6}$$

If the inlet temperature is chosen to be the lithium melting temperature plus a 25°C safety margin, then $T_{MAX} = 96.8 + 28.2 + 25 + 186 = 336°C$ which corresponds to a lithium vapor pressure of 4×10^{-6} torr. The evaporation rate associated with this temperature is to be less than the sputtering rate.

Hydrogen Removal: G. M. McCracken and S. K. Erents[11] report experimental results for the trapping of deuterium in lithium. Trapping efficiencies in the range of 50-96% are achievable for clean lithium surfaces over a large temperature range. The measurements were made for doses up to 2.2×10^{22} ions/m² and show no sign of a saturated lithium-hydride surface. The incident hydrogen-ion flux for ITER is estimated from $\Gamma_p = (n V_p/\tau_p)/(2 N_B L_s H)$, where the particle confinement time, τ_p, is assumed equal to $4\tau_E = 8s$. For a plasma volume, V_p, of 700m³ and $n = 7 \times 10^{19} m^{-3}$, then $\Gamma_p = 3.2 \times 10^{20}$ ions/m²s. For a velocity of $v = 160 m/s$ the total dose per droplet is $1.1 \times 10^{19} m^{-2}$, which can be easily accommodated by the LDB.

From the trapping curves, only about 75% of the beam should be trapped on initial contact. An attractive feature associated with the

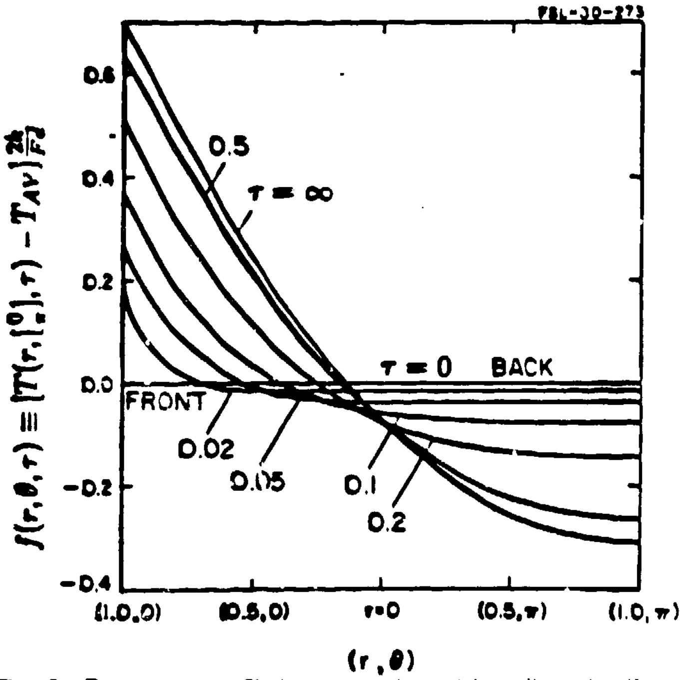

Fig. 5. Temperature profile in a sphere located in a directed uniform heat flux[17] (along the diameter aligned with the direction parallel to the external heat flux). Dimensionless radius and time variables are used.

LDB is the extended lithium surface available for "gettering" hydrogen and impurities. The total surface area of only lithium in the interaction zone of the droplets is $69m^2$, whereas if all the lithium in the interaction zone were combined into a single sphere it would have a surface area of $0.72m^2$. Reflected particles will primarily be located either in the middle of the beam, or in the edge-plasma flow region and, therefore, have a high probability of being trapped. Little experimental work exists on lithium as a pumping material, however, and important unanswered questions remain, some of which are listed below:

1. What is the feasibility for separating lithium-hydride at the required rate and to the required concentrations?
2. Hydrogen re-emission rates for T > 650°C are not known and this restriction could limit temperatures to values lower than the vapor pressure limitation.
3. How well does lithium pump neutral hydrogen isotopes?
4. What is the ability of the droplets to retain helium? If the droplets retain helium sufficiently long to remove it from the reactor chamber, the need for additional He vacuum pumps would be alleviated.

Erosion Rates: The average physical sputtering rate is given by $\dot{S} = \Gamma_p \gamma A_s$, where $\gamma = 0.04$ lithium atoms sputtered per several-hundred-eV incident deuterium atoms. The average lithium vaporization flux rate is given by Dushman,[19] $\Gamma_{ev} = 5.36 \times 10^{15} exp[15.44(T/348 - 1)]$, which has a value of $3.1 \times 10^{19}/m^2s$ at 336°C. For an assumed hot (336°C) area of $0.2\ A_s$, then the ratio of the vaporization rate to the sputtering rate is $\Gamma_p \gamma A_s/(\Gamma_{ev} 0.2 A_s) = 0.26$. Therefore, evaporation should be less serious than sputtering.

The gross physical sputtering rate is $6 \times 10^{19} Li/s$ per beam, which corresponds to an effective yearly gross erosion rate of $4.5mm/yr$ and a fractional erosion per droplet of about 10^{-8}. The net erosion rate should be well below the gross value because of redeposition.

BEAM SIZE AND HYDRODYNAMICS

Temperature Limitations: With a safety margin of 25°C, the minimum system temperature set by the melting point (T_{mp}= 186 °C) is 211°C. The maximum temperature is determined either by the vapor pressure permitted in the plasma chamber or by hydrogen retainability requirements previously discussed. For a peak lithium vapor pressure of $4 \times 10^{-6} torr$, the maximum lithium temperature is 336°C. This is a rather low temperature for achieving good thermal conversion efficiency. If higher temperatures are desired, then a configuration is needed that permits a differential vacuum pumping scheme to decouple the plasma and LDB beam vapor pressure. For instance, a droplet outlet temperature of 500°C results in a vapor pressure of $8 \times 10^{-3}\ torr$, which is an unacceptably high neutral-gas pressure, if adjacent to the core plasma.

Droplet Spacing and Beam Dimensions: The probability of a plasma particle striking the first column of droplets is given by the area ratio $a = \pi d^2/4h\ell cos\theta$ (Fig. 5). Since this ratio is the probability for a plasma particle to hit lithium in moving a distance $w/cos\theta$, the beam attenuation can be approximated as a continuous function characterized by a macroscopic absorption cross section $\Sigma \equiv a/\ell = \pi d^2/4h\ell w$. The lithium volume fraction, ε, is $\pi d^3/6h\ell w$, so $\Sigma = 3\varepsilon/2d$. From photographs[15] of droplet formation, the spacing in the direction of droplet motion is chosen to be $\ell = 1.5d$. The spacing in the other two directions is determined by nozzle array, which is assumed to be $w = h = 2d$. It follows that $\varepsilon = 0.087$ and $\Sigma = 26.2m^{-1}$. Since five mean free paths is sufficient to collect 99.3% of the incident energy, the length of the collection region must be $X = 5/\Sigma = 0.19$ m. This value can be controlled through the droplet size and spacing. The angle between a field line and the area surface vector, $\vec{A}_s$, is conservatively estimated using Figure 6 to be greater than or equal to $\sin^{-1}\frac{3.7}{5.5} = 42.3°$, so a beam width of $W = X \cos\theta = 0.14m$ results.

The beam height, H, is set by the requirement that the heat flux associated primarily with the toroidal direction is intercepted by the LDB. Hence, a field-line that just misses the top of a the LDB must intersect the bottom of the next beam; the following expression for H results: $H \simeq 2\pi R_T B_\theta/(2N_B B_\phi)$. For two beams and $B_\theta/B_\phi = 0.1$ in the divertor region, it follows that $H = 0.86m$.

Lithium Mass Flow Rate and Circulation Power: The mass flow rate is given by $\dot{m} = \rho\ \bar{v}\ AN_B$, where the flow area is given by, $A = DHW \cdot (\pi d^2/4hw)$, and the average fluid speed, $\bar{v}$, is given by

$$\bar{v} = \frac{1}{L}\int_0^L v(x)dx \quad . \tag{11}$$

For a uniform velocity, $\bar{v} = v$. For a double-exponential velocity profile in the interaction region ($v = v_o[e^{-\Sigma x} + e^{-\Sigma(X-x)}]$) which minimizes the mass flow rate subject to temperature limitations, $\bar{v} = 2v_o/\Sigma X$. The mass flow rate, then, is $\dot{m} = 23.6\bar{v} = 3,782kg/s$ for a uniform velocity distribution (with a factor of 0.4 reduction possible for a double-exponential velocity profile). The average force of the beam in the direction of flow is $2.5\ MPa$ (with a factor of 0.13 reduction possible). The kinetic power driving the heat is $\frac{1}{2}v^2\dot{m}$, which equals $48.6\ MW$ for a uniform velocity distribution and $6.5\ MW$ for the double-exponential profile. Clearly, this latter situation is required to keep the circulation power to 3% of the ITER thermal power.

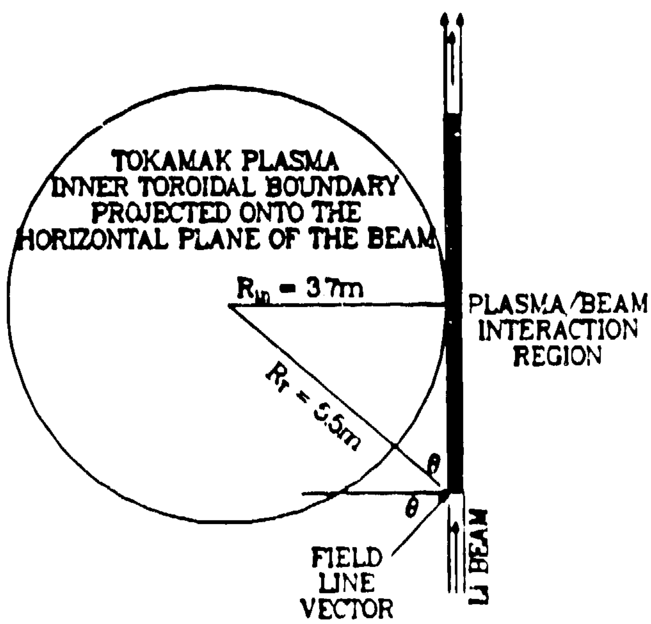

Fig. 6. Geometry used for estimating the angle between the incident plasma heat and particle flux and the normal to the surface of the LDB.

The power required to circulate coolant against frictional losses is given by $P_f = \Delta p_f A v_c$, where v_c is the circulation velocity. The Darcy-Weisbach formula[20] gives the pressure drop: $\Delta p_f = f' Y \rho v_c^2/(2D_e)$. Here, the Darcy-Weisbach friction factor is f', the equivalent diameter is $D_e = (4A/\pi)^{1/4}$, and Y is the piping length. For $v_c = 10 m/s$ A is $0.047 m^2$ and D_e is $0.245 m$. The Reynolds number, then, is Re = 3×10^6, and from the Moody chart[20], $f' = 0.0096$ for a smooth pipe. Hence, for $Y = 30m$, $P = 14kW$ which corresponds to 0.006% of the ITER thermal power carried by the lithium.

SUMMARY AND CONCLUSIONS

Table III summarizes the LDB divertor collector parameters as applied to ITER for both constant and double-exponential velocity profiles. The exponential velocity profile is desirable, since it lowers the mass flow rate; the constant-velocity case projects acceptable design values, except for the high circulation power.

TABLE III. Sample LDB Parameters for ITER Conditions

Volume fraction of lithium in collection zone, ε	0.087
Beam width, $W(m)$	0.14
Beam height, $H(m)$	0.86
Beam length, $L_B(m)$	30
Length of collection zone, $L_e(m)$	5.5
Droplet diameter, $d(m)$	0.005
Velocity profile, v	v_o; $(v_o[e^{-\Sigma x} + e^{-\Sigma(X-x)}])$
Maximum droplet velocity, $v_o(m/s)$	160 (160)
Average droplet velocity, $\bar{v}(m/s)$	160 (64)
Jet break-up length, $b(m)$	2
MHD droplet velocity reduction, $\Delta v(m/s)$	0.011
MHD sidewards deflection, $\Delta y(m)$	10^{-10}
Gravitational deflection, $\Delta z(m)$	0.043
MHD deformation pressure drop, $\Delta p(N/m^2)$	876
Lithium surface tension, $p_s(N/m^2)$	292
Lithium inlet temperature, $T_{IN}(°C)$	211
Peak lithium outlet temperature, $T_{MAX}(°C)$	336
Average temperature increase per droplet $\Delta T_{AV}(°C)$	28.2
Peak lithium vapor pressure, $(torr)$	4×10^{-6}
Gross physical sputtering rate, $\dot{\delta}_{sp}(mm/yr)$	4.5
Gross evaporation rate, $\dot{\delta}_{ev}(mm/yr)$	1.2
Extended lithium surface area, $A_{L_i}(m^2)$	69
Mass flow rate, $\dot{m}(kg/s)$	3,800 (1,520)
Lithium recirculation power, $P(MW)$	49 (6.5)
Frictional power loss, $P_f(MW)$	0.014
ITER Parameters:	
Major toroidal radius $R_T(m)$	5.8
Fusion power, $P_F(MW)$	670
Radiation fraction, f_{RAD}	0.3
Particle throughput, $\dot{S}_p(particle/s)$	6.1×10^{21}

A LDB system configuration has been described that requires only a small fractional volume of the ITER device and for the present ITER base case would appear to fit through the magnets. Estimation of the LDB size give reasonable parameters, but 2 and 3-D equilibrium calculations and field line tracings are necessary to vary the equilibrium and to ensure that both the inboard and outboard diverted field lines are intercepted by the beam. A range of alternative configurations can be envisioned. Vertical beams would eliminate gravitational deflection concerns and shorten the beam length such that slower droplet speed could be permitted. Additional beams (more than 2) should reduce the beam height, H, and the power collected per droplet, which would also reduce beam speed requirements. Based on individual droplet considerations, no major faults have been identified with the LDB concept. Droplets can be formed, can traverse the required distances and collect heat and particles. The liquid-droplet concept eliminates thermal and pressure stress associated with a solid plate and eliminates maintenance concerns inside the reactor chamber. Also, the moving droplets reduce, if not eliminate, any problems associated with hot spots from uneven heat fluxes. For ITER, however, the LDB concept operates near a limit in total energy removed per droplet. A 160 m/s droplet speed is large. Perhaps the vertical beam configuration suggested above, which would have a shorter vertical path length and more beams, could handle a larger or higher total power design. More work is required to understand the droplet deformation effects caused by the $\vec{J} \times \vec{H}$ force.

The lithium mass flow rate is large, but manageable, and could be reduced by some of the above-mentioned system configurational changes. It is noted that the present work only provides an approximate LDB design. A more precise design would require improved descriptions of the LDB configurations, the magnetic geometry, and the edge-plasma conditions.

In conclusion, the lithium jet energy-particle collection scheme has many distinct advantages over a solid collector plate, with no obvious major problems. These features are summarized in Table I. More experimental data are needed on droplet formation, collection, and particle pumping. A lithium beam could be built today for testing purposes.

REFERENCES

1. "ITER Concept Definition," report ITER-I, (October 1988).
2. T. F. Yang, A. Y. Lee, and G. W. Ruck, "Westinghouse Compact Poloidal Divertor Reference Design," WFPS-TME-042, Westinghouse Fusion Power Systems Department, Pittsburgh, Pennsylvania (August 1977).
3. "UWMAK I: A Wisconsin Toroidal Fusion Reactor Design," p. III-D-1, UWFDM-68 (revised ed.), University of Wisconsin, Madison, Wisconsin (1974).
4. W. M. Wells, "Lithium Particle and Energy Collection System" internal correspondence Fusion Reactor Engineering Dept.of Union Carbide, Oak Ridge, Tenn., (July 11, 1978).
5. W. M. Wells, "Lithium Droplet Divertor Collection for Ions and Heat," Proc. 8th Symp. on Eng. Problems of Fusion Research, SF, CA (1979).
6. R. L. Reid, W. M. Wells, et al., "Oak Ridge TNS Program: System Description Manual," ORNL/TM-6721, 45 (May 1979).
7. K. A. Werley, "Design Considerations for a Steady State Fusion Reactor's Thermal Energy Dump (TED) with Emphasis on SAFFIRE," Masters Thesis in Nuclear Engineering, U. of Illinois (1980).
8. K. A. Werley, J. G. Gilligan and G. H. Miley,"A High Flux Energy and Particle Collection Scheme for Divertors," 11th Symposium on Fusion Technology, DP. 1-13, Oxford, England (1980).
9. K. A. Werley and J. G. Gilligan, "Lithium Rain Particle-Energy Collection Scheme," U. of Illinois Nuclear Engineering Report EPRI-AFR-137 (1980).
10. E. V. Murav'ev, "Questions of Atomic Science and Engineering, Series on Thermonuclear Fusion," [in Russian], (1980), No. 2(6), p. 57.
11. E. V. Murav'ev, "Proceedings of the Third All-Union Conference on Engineering Problems of Fusion Reactors," [in Russian], Vol 4 (1984), p. 49.
12. A. V. Tananaev, E. V. Murav'ev, and V. V. Yakovlev, "Proceedings of the Third All-Union conference on Engineering Problems of Fusion Reactors," [in Russian], Vol. 4 (1984), p. 187.
13. V. O. Vodyanyuk, V. N. Dem'yanenko, A. F. Kolesnichenko, S. V. Mirnov, E. V. Murav'ev, E. K. Sergeev, and A. M. Shapiro, "Liquid-metal Tokamak Limiter: Statement of The Problem and First Results," *Sov. J. Plasma Phys.* **14** (5), (May 1988), p. 370.
14. Tiu-Fang Chen and J. R. Davis, "Disintegration of a Water Jet," *ASCE J. Hyd. Div.*, **90**, no. 103, 182 (1964).
15. R. E. Phinney, "The Breakup of a Turbulent Liquid Jet in a Gaseous Atmosphere," *J. Fluid Mech.*, Vol. 679, part 4, 689 (1973).
16. J. S. Walker and W. M. Wells, "Drag Force on a Spherical Drop in a Non-uniform Magnetic Field," ORNL/TM-6976, Oak Ridge, TN (1979).
17. K. A. Werley and J. G. Gilligan, "The Temperature Distribution of a Sphere Placed in a Directed Uniform Heat Flux," *Trans. of the ASME, J. Heat Transfer*, **103**, No. 2, 399 (May 1981).
18. G. M. McCracken and S. K. Erents, "Ion Burial in the Divertor of a Fusion Reactor," BNES Nuclear Fusion Reactor Conference, Culham, (September 1969).
19. S. Dushman, Scientific Foundation of Vacuum Technique, John Wiley, New York, 1940.
20. R. M. Olson, Essentials of Engineering Fluid Mechanics, Intext Press, Inc., New York, 1973.